JPn Neuroscience

The Journal of Physiology

J Physiol 592.4 (2014) pp 729–743

Modulation of stimulus-specific adaptation by $GABA_A$ receptor activation or blockade in the medial geniculate body of the anaesthetized rat

Daniel Duque[1,2], Manuel S. Malmierca[1,3] and Donald M. Caspary[2]

[1]*Auditory Neurophysiology Unit, Laboratory for the Neurobiology of Hearing, Institute of Neuroscience of Castilla y León, University of Salamanca, Salamanca, Spain*

[2]*Department of Pharmacology, Southern Illinois University School of Medicine, Springfield, IL, USA*

[3]*Department of Cell Biology and Pathology, Faculty of Medicine, University of Salamanca, Salamanca, Spain*

Key points

- Neurons in the medial geniculate body (MGB), the auditory thalamus, give stronger responses to rare sounds than to repetitive sounds, a phenomenon referred to as stimulus-specific adaptation (SSA).
- The present study sought to elucidate how the inhibitory thalamic circuitry acting at $GABA_A$ receptors affects the generation and/or modulation of SSA from recordings of single unit responses from MGB. Microiontophoretic application of GABAergic agonists selectively increased SSA indices, whereas application of antagonists selectively reduced SSA values.
- We found that $GABA_A$-mediated inhibition did not generate the SSA response but regulated the magnitude of SSA sensitivity in a gain control manner.
- These findings advance our understanding of the role of inhibition in coding deviance detection in the MGB.

Abstract Stimulus-specific adaptation (SSA), which describes adaptation to repeated sounds concurrent with the maintenance of responsiveness to uncommon ones, may be an important neuronal mechanism for the detection of and attendance to rare stimuli or for the detection of deviance. It is well known that GABAergic neurotransmission regulates several different response properties in central auditory system neurons and that GABA is the major inhibitory neurotransmitter acting in the medial geniculate body (MGB). The mechanisms underlying SSA are still poorly understood; therefore, the primary aim of the present study was to examine what role, if any, MGB GABAergic circuits play in the generation and/or modulation of SSA. Microiontophoretic activation of $GABA_A$ receptors ($GABA_A$Rs) with GABA or with the selective $GABA_A$R agonist gaboxadol significantly increased SSA (computed with the common SSA index, CSI) by decreasing responses to common stimuli while having a lesser effect on responses to novel stimuli. In contrast, $GABA_A$R blockade using gabazine resulted in a significant decrease in SSA. In all cases, decreases in the CSI during gabazine application were accompanied by an increase in firing rate to the stimulus paradigm. The present findings, in conjunction with those of previous studies, suggest that $GABA_A$-mediated inhibition does not generate the SSA response, but can regulate the level of SSA sensitivity in a gain control manner. The existence of successive hierarchical levels of processing through the auditory system suggests that the GABAergic circuits act to enhance mechanisms to reduce redundant information.

DOI: 10.1113/jphysiol.2013.261941

(Received 11 July 2013; accepted after revision 6 October 2013; first published online 7 October 2013)
Corresponding author D. M. Caspary: Department of Pharmacology, Southern Illinois University School of Medicine, 801 North Rutledge, Springfield, IL 62702, USA. Email: dcaspary@siumed.edu

Abbreviations MGB, medial geniculate body; SSA, stimulus-specific adaptation; CSI, common SSA index; FRA, frequency response area; GABA, γ-aminobutyric acid.

Introduction

An optimal response to new acoustic information in the presence of continuous sounds is critical for animal survival. In the central auditory system, many neurons adapt to repeated sounds while maintaining responsiveness to uncommon ones, allowing the detection of rare sounds in an otherwise monotonous auditory scene. This phenomenon is referred to as stimulus-specific adaptation (SSA) (Ulanovsky *et al.* 2003) and has been found from the inferior colliculus (IC) (for a review see Ayala & Malmierca, 2013) through to the auditory cortex (AC) (Ulanovsky *et al.* 2003, 2004; von der Behrens *et al.* 2009; Taaseh *et al.* 2011; Yaron *et al.* 2012). SSA is also present in the anaesthetized (Anderson *et al.* 2009; Yu *et al.* 2009; Antunes *et al.* 2010; Antunes & Malmierca, 2011) and the unanaesthetized (Richardson *et al.* 2013*a*) medial geniculate body (MGB), and has been confirmed as strong and widespread in the non-lemniscal pathway (Malmierca *et al.* 2009; Antunes *et al.* 2010; Duque *et al.* 2012). The mechanisms underlying SSA are poorly understood and the role of the inhibitory circuitry in the generation and/or modulation of SSA in the auditory thalamus remains to be delineated.

The MGB in the auditory thalamus is essential for relaying, processing, filtering and attending to acoustic information. It consists of three main divisions: the ventral (MGV), dorsal (MGD) and medial (MGM). The MGV forms the lemniscal division, and the MGD and MGM are each part of the non-lemniscal pathway, which is related to the analysis of complex features of sound and multisensory integration (for reviews, see Winer, 1985; Hu, 2003; Lee & Sherman, 2011). Synaptic and extrasynaptic inhibition in the MGB is primarily mediated by GABA acting at both $GABA_A$ and $GABA_B$ receptors (Bartlett & Smith, 1999; Richardson *et al.* 2011) because MGB lacks glycinergic receptors (Aoki *et al.* 1988; Friauf *et al.* 1997). GABAergic interneurons are virtually absent in the rat MGB (only ~1%) (Winer & Larue, 1996; Bartlett & Smith, 1999), but the MGB receives significant GABAergic projections from the IC (Winer *et al.* 1996; Peruzzi *et al.* 1997; Ito *et al.* 2011) and the thalamic reticular nucleus (TRN) (Rouiller *et al.* 1985), the two major sources of GABAergic inhibition to the MGB. The GABAergic inputs to the MGB are known to shape the frequency response areas (FRAs) and adjust thresholds of MGB neurons (Suga *et al.* 1997; Cotillon-Williams *et al.* 2008).

As Pérez-González and colleagues (2012) have described a gain control role for the inhibitory circuitry of the IC and Yu *et al.* (2009) have suggested that the GABA inputs to the MGB shape the novelty response, the present study was designed to shed light on the possible role of $GABA_A$ receptor ($GABA_AR$)-mediated inhibition in the generation of SSA in the MGB of the rat. Microiontophoresis was used to reversibly block or activate $GABA_ARs$ during oddball paradigm stimulation concurrent with recording from well-isolated single units in the MGB. We recorded before, during and after application of: (i) the $GABA_AR$ endogenous agonist GABA; (ii) the subunit-selective $GABA_AR$ agonist gaboxadol, and (iii) the $GABA_AR$ antagonist gabazine. Our results demonstrate that gabazine increased firing rate and decreased the magnitude of SSA, whereas GABA and gaboxadol produced the opposite effect, such that firing rates decreased and the degree of SSA increased. These results support the suggestion that the GABAergic system in MGB does not shape the SSA response, but exerts a modulator gain control effect.

Methods

Ethical approval

All experimental procedures were carried out in accordance with protocols approved by the Laboratory Animal Care and Use Committee of Southern Illinois University School of Medicine (SIU Animal Protocol Number: 41-10-002).

Surgical procedures

Experiments were performed on 23 4-month-old, male Fischer Brown Norway rats. Rats were initially anaesthetized with I.M. injection (1.4 ml kg^{-1}) of a ketamine-HCl (100 mg ml^{-1}) and xylazine (20 mg ml^{-1}) mixture. Anaesthesia was maintained by I.P. injections of urethane [initially 1.3 ml kg^{-1}, then one-third of the initial amount in booster doses; 750 mg kg^{-1} (Sigma-Aldrich Corp., St Louis, MO, USA)]. Urethane was chosen as an anaesthetic agent because it acts on multiple neurotransmitter systems rather than simply potentiating the effects of inhibitory systems, and its effects are thought to be less problematic than those generated by barbiturates and/or other anaesthetic agents (Hara & Harris, 2002).

Body temperature was maintained at $37 \pm 0.5^{\circ}$C by a thermostatically controlled heating blanket. Rats were placed in a stereotaxic frame with a customized jaw bar and head holders inside a double-walled, sound-proofed booth (Industrial Acoustic Co., Inc., New York, NY, USA). Prior to surgery, auditory brainstem responses (ABRs) to click and 4 kHz, 8 kHz, 16 kHz and 32 kHz tones (3 ms duration, 1 ms ramp, 20 s^{-1} rate) were obtained to check that the animal had normal hearing. ABR recordings were obtained as previously described (Wang *et al.* 2009) using a vertex electrode and subcutaneous electrodes in the nose (reference) and neck (ground). Signals were amplified 500,000 times and averaged over 512 trials with hearing thresholds determined visually. None of the animals used in these experiments showed any signs of hearing loss.

Acoustic stimuli and electrophysiological recording

A craniotomy was performed to expose the cerebral cortex (5.5 mm from the bregma, 3.5 mm laterally from the midline) over the centre of the MGB (Paxinos & Watson, 2007). Extracellular single unit responses were recorded using a six-barrel carbon fibre microelectrode (carbon fibre: >0.8 MΩ, Carbostar-6; Kation Scientific, Minneapolis, MN, USA). Custom software (ANECS, Ken Hancock; Blue Hills Scientific, Boston, MA, USA) controlled Tucker-Davis Technologies (TDT) System III hardware to generate acoustic signals. The signal was amplified (TDT, ED1), transduced (TDT, EC1) and delivered to the right ear canal using polypropylene tubing. The sound system was calibrated offline into a simulated rat ear (Caspary *et al.* 2005) using a $\frac{1}{4}$ inch microphone (Bruel & Kjaer, model 4938). Pure tone intensities in dB SPL (sound pressure level) were accurate to ± 2 dB for frequencies up to 45 kHz (Caspary *et al.* 2005). Search stimuli were 70–80 dB broadband noise pips. Spike output from the carbon fibre was led to a single channel of a 16-channel unity-gain headstage tethered to a pre-amplifier [2× gain, 0.15 kHz (high pass), 8 kHz (low pass); Plexon, Inc., Dallas, TX, USA]. Spikes were digitized and visualized using Sort Client, with action potentials/spikes sorted using amplitude threshold and saved as timestamps (Plexon, Inc.).

Stimulus presentation paradigms

Upon isolating a unit, the approximate frequency response was manually determined by presenting tone-bursts (100 ms duration, 5 ms rise/fall time, four bursts/s rate). Automated FRAs were then obtained using random combinations of frequencies and intensities evoking a response resulting in a mapped neuronal receptive field. Pure tones were presented using an automated procedure with five stimulus repetitions at each frequency (0.5–40 kHz, in 20–30 logarithmic steps) and intensity (10 dB SPL intensity steps, 0–80 dB SPL) point. Higher-resolution response maps were used to more accurately determine characteristic frequency (CF) as needed. A collection window was set to count the spike number during the response of the neuron (typically 100 ms in duration). Minimum thresholds and best frequency (BF) (i.e. the frequency that evoked a response with the lowest intensity) responses were derived from these maps.

The oddball paradigm was used to evaluate SSA. The calculation of the FRA allowed selection of frequency pairs (f_1 and f_2) that elicited similar firing rates at the same stimulus level. Each frequency in the pair was always presented at the same sound level. Stimuli presented in an oddball paradigm were similar to those used to record mismatch negativity responses in human (Näätänen, 1992) and SSA responses in animal (Ulanovsky *et al.* 2003, 2004; Malmierca *et al.* 2009; Antunes *et al.* 2010; Duque *et al.* 2012; Ayala *et al.* 2013; Richardson *et al.* 2013*a*) studies. Briefly, 300 stimuli containing both frequencies were presented in a probabilistic manner: one frequency (f_1) presented as a standard sound (90% of occurrence) was interspersed randomly with a second deviant (10% of occurrence) stimulus frequency (f_2). After recording responses, the relative probabilities of the two stimuli were reversed. Dot raster plots were used to visualize responses obtained to the oddball paradigm by plotting individual spikes (each dot is a spike: red dots indicate responses to the deviant; blue dots indicate responses to the standard). Presentations were marked along the vertical axis. As the pairs of frequencies were chosen close to the threshold (where the FRA is narrower), the frequency contrast was set at $\Delta f \approx 0.10$, where $\Delta f = (f_2 - f_1)/(f_2 \times f_1)^{1/2}$ (Ulanovsky *et al.* 2003, 2004; Malmierca *et al.* 2009). The average stimulus intensity was 17.26 ± 11.97 dB above the CF threshold. Stimuli were presented at a rate of four per second, conditions previously shown to evoke strong SSA in the MGB (Antunes *et al.* 2010; Antunes & Malmierca, 2011).

SSA responses were quantified by computing the common SSA index (CSI) (Ulanovsky *et al.* 2003), defined as $\mathrm{CSI} = [\mathrm{d}(f_1) + \mathrm{d}(f_2) - \mathrm{s}(f_1) - \mathrm{s}(f_2)] / [\mathrm{d}(f_1) + \mathrm{d}(f_2) + \mathrm{s}(f_1) + \mathrm{s}(f_2)]$, where $\mathrm{d}(f)$ and $\mathrm{s}(f)$ are responses to each frequency f_1 or f_2 according to whether they represented a deviant (d) or standard (s) stimulus. CSI reflects the extent to which the response to the standard was suppressed. CSI values range between -1 and $+1$; more positive values reflect a greater response to the deviant stimulus. We used the CSI value of 0.18, defined by Antunes *et al.* (2010), as the threshold for significant SSA. This cut-off value was established by choosing the most negative CSI value in the dataset (-0.18) to represent the most extreme variance due to random fluctuations in spike counts. For consistency and to enable comparisons, we applied the same value as

used previously. To minimize the effects of spontaneous activity in the analysis, collection time windows were chosen individually for each unit. The default time window embraced the whole stimulus (0–100 ms) for low spontaneous activity responses (e.g. Fig. 2*A*). For cases of high spontaneous activity (e.g. Fig. 2*B*), time windows were set based on the shape of the peristimulus time histogram (PSTH) (i.e. by focusing or narrowing the window around the peak of the response. SSA was also quantified by calculating the frequency-specific index $SI(f_i)$, where $i = 1$ or 2, defined for each frequency f_i as $SI(f_i) = [d(f_i) - s(f_i)] / [d(f_i) + s(f_i)]$, where $d(f_i)$ and $s(f_i)$ are responses to frequency f_i when it is deviant or standard, respectively.

Iontophoresis and pharmacology

When the MGB was located, iontophoretic studies were performed using the six-barrel Carbostar multibarrel electrode. A current-balancing barrel was filled with 2 M potassium acetate and the remaining barrels were filled with drugs purchased from Sigma-Aldrich Corp. These included the $GABA_AR$ endogenous agonist γ-aminobutyric acid (GABA; 500 mM, pH 4.0), the $GABA_AR$ subunit-selective superagonist gaboxadol (10 mM) and the $GABA_AR$ antagonist gabazine (10 mM). Iontophoretic current was supplied by a multi-channel iontophoresis system (BH-2 Neuro-Phore System; Harvard Apparatus/Medical Systems, Inc., Holliston, MA, USA) through a silver chloride wire and was generally kept at 0–100 nA to avoid excessive diffusion (Foeller *et al.* 2001). Candy *et al.* (1974) have shown that certain small molecules, iontophoretically delivered agents, which are not rapidly removed, can diffuse up to 600 μm. In the rat MGB, this range would cover most of the extent of the dendritic arbours (MGV: ~280 μm; MGD: ~400 μm; MGM: ~750 μm) (Clerici *et al.* 1990; Bartlett & Smith, 1999; Smith *et al.* 2006). However, we cannot exclude the possibility that agents used here may have affected GABA receptors located at more distant dendritic branches. Recording and iontophoretic procedures were similar to those described elsewhere (e.g. Backoff *et al.* 1999; Caspary *et al.* 2002; Pérez-González *et al.* 2012). A full return to baseline/pre-drug level was set, regardless of the time, before additional agents were applied. For each unit studied, the dose and time of application were varied (0–100 nA, 1–20 min) with the aim of achieving a steady state level of drug action.

Data analysis

Statistical tests were performed using the multiple non-parametric Friedman signed rank test to test differences between distribution medians of varying conditions. *Post hoc* comparisons were performed following Dunn's method. Statistical tests were considered significant when $P < 0.05$. The S.D. for the CSI and the firing rate of each individual neuron were calculated using bootstrapping (1000 repetitions). The limits of 95% confidence intervals (CIs) were calculated using the 2.5 and 97.5 percentiles of the CSI bootstrap distribution obtained for each neuron; the 5% confidence level was used to determine statistically significant differences in the CSI and firing rate values between conditions. Analyses and figures were executed using Sigmaplot Version 11 (Systat Software, Inc., Chicago, IL, USA) and Matlab (MathWorks, Inc., Natick, MA, USA).

Histological verification

At the end of each experiment, the animal was perfused with buffered saline followed by 4% paraformaldehyde and decapitated. The brain was removed and placed in 20% sucrose overnight. The brain was blocked and 50 μm coronal sections were stained with fast thionin. The depth for recording each unit was carefully recorded. As the track left by the Carbostar electrode was readily visible, the need for lesion or dye injection was obviated. Tracks were localized using a rat brain atlas (Paxinos & Watson, 2007) and previous MGB studies (Bartlett & Smith, 1999; Antunes & Malmierca, 2011).

Results

To study the impact of GABAergic inhibition on SSA sensitivity, we recorded responses to an oddball stimulus paradigm from 52 well-isolated single units throughout the MGB, before, during and after application of gabazine, GABA and gaboxadol. Generally, microiontophoretic application of gabazine increased firing rates and reduced SSA levels, whereas the application of GABA and gaboxadol produced an opposite effect. The detailed effects that $GABA_AR$-related agents produce on firing rate, SSA indices, dynamics of adaptation and latency were evaluated separately.

SSA in the MGB

As expected from previous reports (Antunes *et al.* 2010), a majority of neurons sampled showed significant SSA [42 of 52 neurons (81%), CSI > 0.18] (i.e. they responded preferentially to a deviant tone compared with the commonly occurring standard). Across the population, the full range of CSI values (−0.001 to 0.897; mean ± S.D. 0.443 ± 0.249; $n = 52$) was observed (Fig. 1*A*). To test the possibility of a differential drug effect over the two frequencies analysed, we checked whether there was any preference for the deviant stimulus according to whether the deviant was presented as f_1 or f_2. The analysis of SI values

confirmed that the majority of values were positive and located in the upper right quadrant ($n = 104$; mean ± S.D. 0.403 ± 0.325; one-sample t test, $P \leq 0.001$) (Fig. 1*B*). The Mann–Whitney rank sum test confirmed there were no differences in the population between SI_1 and SI_2 values ($P = 0.241$).

Recording sites were localized from histological sections according to the track marks through the MGB; when possible, a neuron was assigned a position based on known depth in one of the three main MGB divisions. Nine tracks in eight rats were well localized. In five rats, in which 11 units were recorded, tracks were assigned to the MGD and MGM. All neurons from the MGD and MGM showed significant SSA. In the other three rats, tracks were localized in the MGD and MGV and yielded six units. Of these, three units exhibited significant SSA and the remaining three lacked SSA. Thus, only 17 of the 52 (33%) recorded units could be accurately localized, but these data support previous findings that SSA is biased towards the non-lemniscal regions of the MGB, where SSA is strong.

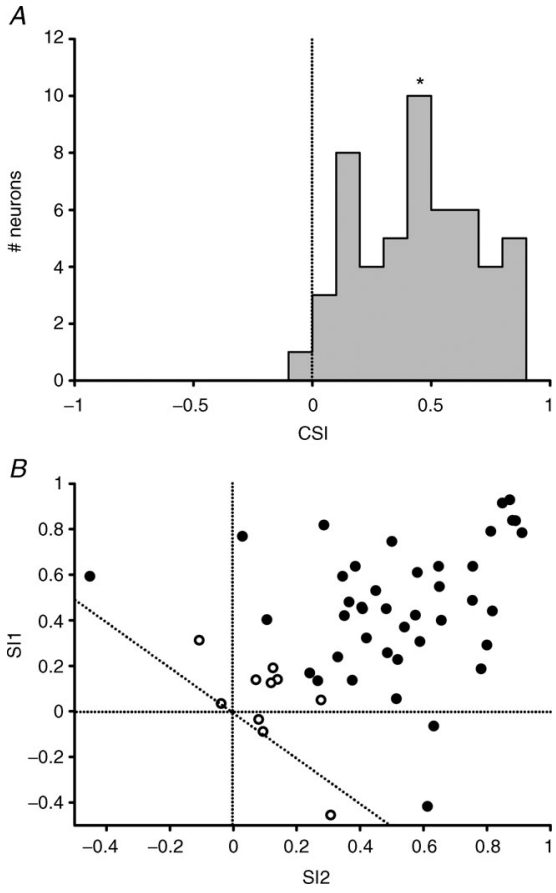

Figure 1. Population data from medial geniculate body (MGB) recordings ($n = 52$) under control conditions
A, histogram of common stimulus-specific adaptation index (CSI) values for the MGB population. *, median CSI value. *B*, scatterplot of frequency-specific index (SI_1 *vs.* SI_2) values for the MGB population. Data lie generally above the diagonal of equal values (black dotted line). Filled dots show neurons with a CSI value higher than the cut-off (CSI > 0.18); empty dots show neurons with a CSI lower than the cut-off (CSI < 0.18).

Effects of gabazine and GABA on firing rate and SSA

The application of gabazine and GABA resulted in profound changes in firing rate and SSA in most MGB neurons. Figure 2 illustrates two examples from individual neurons with corresponding FRAs. The two black dots in the FRAs indicate the frequencies used for the oddball paradigm. Dot raster plots were obtained for four conditions: (i) control; (ii) during gabazine application; (iii) during GABA application, and (iv) during recovery following drug application. The corresponding mean PSTHs for both oddball paradigms are shown below the dot raster plots. The PSTHs of adapting frequency pairs exhibit greater responses to deviant sounds (red line), whereas non-adapting pairs have similar responses to both conditions (red and blue lines at the same level). Figure 2*A* shows a neuron that lacks SSA ($CSI_{control}$: 0.159). Gabazine application produced a 96% increase in firing rate (Fig. 2*A*, PSTH second column) while slightly lowering the CSI ($CSI_{gabazine}$: 0.123). GABA application produced the opposite effect, decreasing firing rate (42% decrease in the control response) (Fig. 2*A*, PSTH third column) while significantly increasing the CSI (CSI_{GABA}: 0.412). Another neuron exhibited a high level of SSA ($CSI_{control}$: 0.528), with the application of gabazine resulting in an 80% increase in firing rate (Fig. 2*B*, PSTH second column) while significantly decreasing CSI ($CSI_{gabazine}$: 0.375). Conversely, GABA reduced the discharge rate by 65% (Fig. 2*B*, PSTH third column) while significantly increasing the CSI (CSI_{GABA}: 0.815). For both neurons cited in Fig. 2, GABA application appeared to suppress the standard relative to the deviant (see also Fig. 3*B*).

Fifty-two neurons recorded from MGB were evaluated for drug responses to establish whether: (i) gabazine application generated a significant increase in firing rate ($n = 40$); (ii) GABA application significantly reduced firing rate ($n = 42$), or (iii) both. Although the increase or decrease in the firing rate response between f_1 and f_2 was correlated (Spearman's rank order correlation, $P < 0.05$ for both standard and deviant responses), the drug effects on both frequencies were analysed separately because a change in firing rate response for a frequency does not necessarily imply the change in the other frequency (52 neurons, 104 frequencies). Conventional responses to the application of $GABA_AR$ agonists or antagonists indicated that responses to the standard tended to be

more affected by $GABA_AR$ manipulation than responses to the deviant. This was the case for gabazine (response increase, standard: 87.73%; deviant: 41.66%; paired *t* test, $Z = -3.036$, $P = 0.002$), and was especially evident in the responses to GABA application in Fig. 3*B* (response decrease, standard: 72.09%; deviant: 54.10%; paired *t* test, $Z = -4.085$, $P < 0.001$). The differential effect of GABA application on the standard, relative to the deviant, is

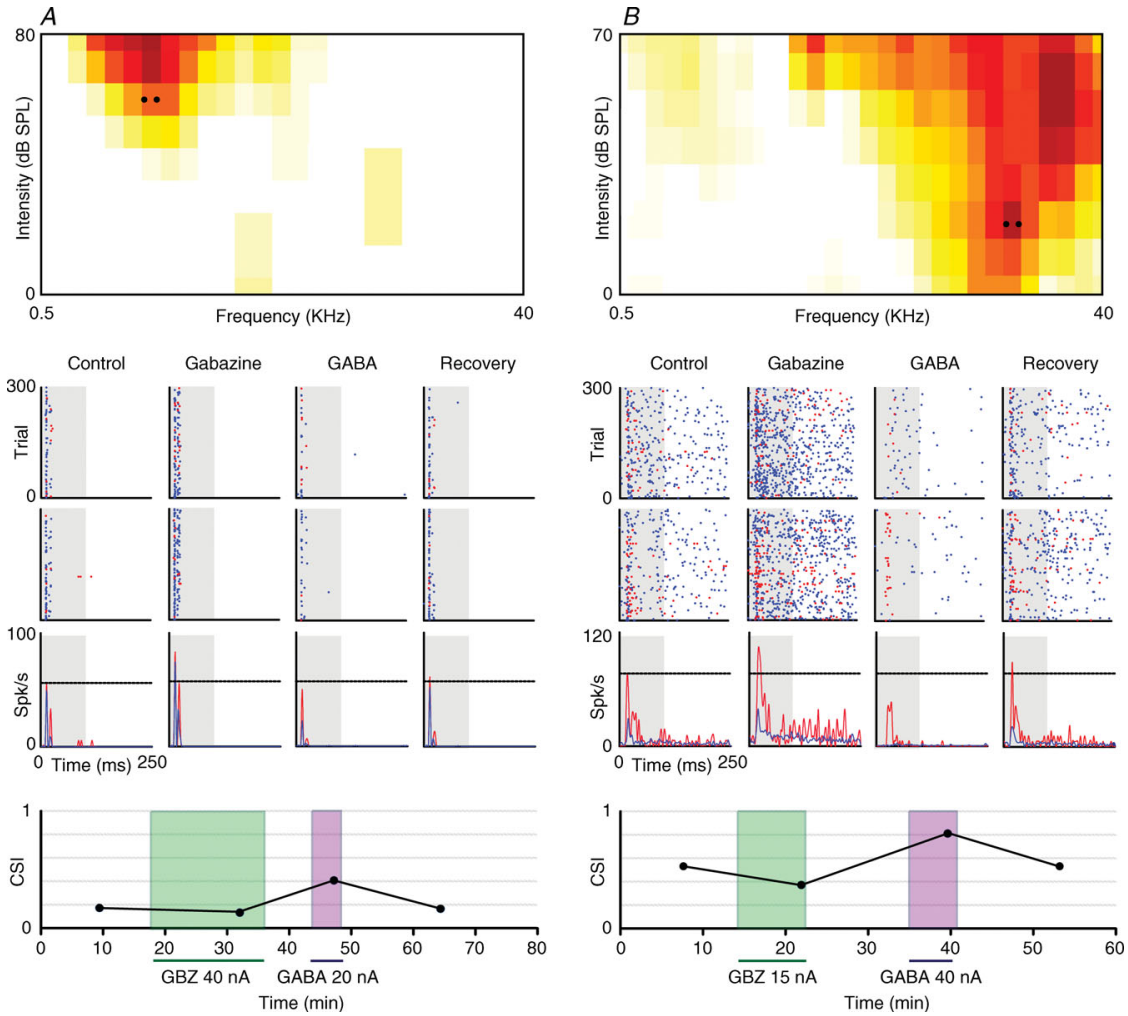

Figure 2. Examples of single unit responses in the medial geniculate body (MGB) before, during and after the application of gabazine and GABA
A, frequency response area (FRA) of a neuron in the MGB that did not show a high common stimulus-specific adaptation (SSA) index (CSI) value in the control condition. *B*, FRA of a neuron in the MGB that showed a high CSI value in the control condition. Black dots over the FRAs represent the pair of frequencies selected for analysing SSA. Below the FRAs, dot raster plots refer to each of the four conditions [control, gabazine (GBZ), GABA and recovery] in the first row (f_1/f_2 as standard/deviant) and the reverse condition (f_2/f_1 as standard/deviant) in the second row. Stimulus presentations are accumulated in the temporal domain in the vertical axis. Blue dots represent spikes evoked by the standard stimulus (90% probability); red dots represent those evoked by the deviant stimulus (10% probability). The time between trials (250 ms; *x*-axis) corresponds to the stimulus repetition rate (4 Hz; with 75 ms stimulus duration). The shadow backgrounds in the dot rasters indicate the duration of the stimulus. Below the dot rasters (third row), peristimulus time histograms (PSTHs) show averaged responses for both frequencies when deviant (red) or standard (blue). The dashed horizontal line in the PSTH shows the deviant peak control response. Lower graphs show the evolution of CSI values during the application of the different drugs. In both examples, neurons in the recovery condition returned to the CSI level of the control/pre-drug condition.

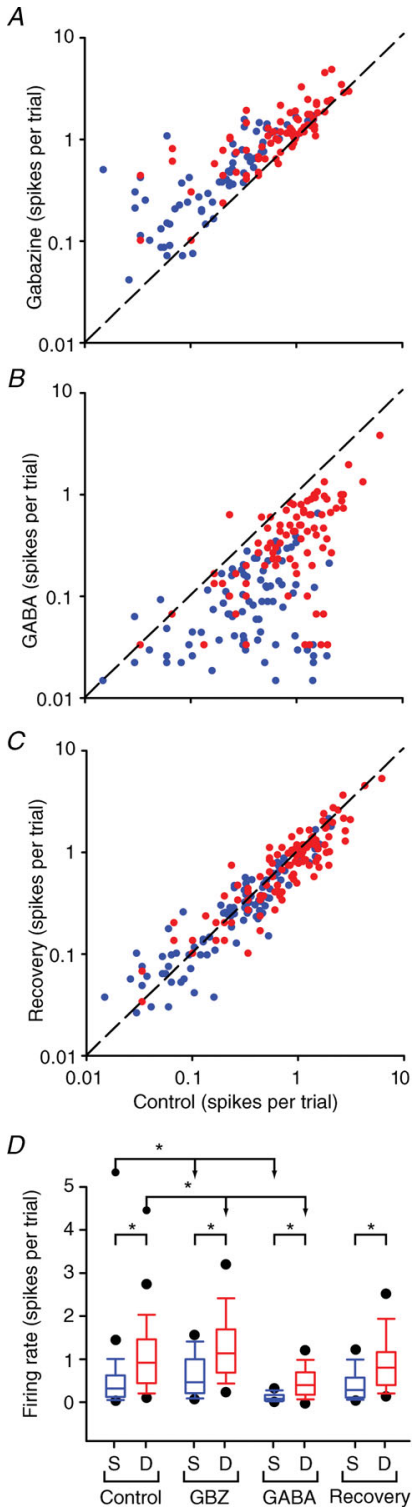

shown in Fig. 3*B* by the cluster of blue dots (standard) below the diagonal line, relative to the number of red dots (deviant) below the diagonal line. In a few cases ($n = 9$) we noted paradoxical effects that depended on the frequency used for stimulation (f_1 or f_2) or the nature of stimuli (standard or deviant), whereby gabazine slightly decreased the response to one frequency (five dots under the diagonal dashed line, Fig. 3*A*) or GABA increased it (four dots over the diagonal dashed line, Fig. 3*B*). These paradoxical effects may occur through small changes in the membrane potential that drive the MGB neuron into burst or tonic mode. In order to evaluate the effects of gabazine and GABA, we used the bootstrap method over 1000 randomizations to estimate the 95% CI of the firing rate response for each neuron in the control condition (data not shown). Then, the firing rates obtained for the gabazine, GABA and recovery conditions for each neuron were compared with the 95% CI firing rate generated for the control condition. We accepted: (i) the finding for gabazine if it presented a firing rate higher than the 95% CI in the control condition; (ii) the finding for GABA if it showed a firing rate lower than the 95% CI in the control condition, and (iii) the finding for the recovery condition if the firing rate response in that condition lay within the 95% CI of the control condition (Fig. 3*C*). (Note that charts *A*–*C* in Fig. 3 are logarithmic. We used this rather than a linear representation to stretch the data that would have been clustered near the origin.) Therefore, at the population level, the firing rates evoked by both the standard and the deviant stimuli were significantly higher when gabazine was applied (Fig. 3*D*, $n = 80$) and lower when GABA was applied (Fig. 3*D*, $n = 84$). Findings in the control condition ($n = 104$) were also compared with those in the recovery condition ($n = 88$). A summary of firing rates obtained in each condition is shown in Table 1. Friedman's repeated-measures ANOVA on ranks found that median values for the standard stimuli differed

Figure 3. Effects of gabazine and GABA on firing rate in the medial geniculate body (MGB) population
A–*C*, scatterplots of the responses (spikes/stimulus) of all neurons to the deviant (red dots) and standard (blue dots) stimuli in the control *vs.* gabazine (*A*), GABA (*B*) and recovery (*C*) conditions. Dots represent one of each frequency analysed separately in every pair of stimuli recorded with the oddball paradigm (52 neurons; 104 frequencies). *A*, gabazine differentially increases the response rate to common/standard stimuli and has a smaller effect on the response rate to novel stimuli. *B*, GABA decreases the response in almost all neurons, having a greater effect on responses to common than to novel stimuli. *C*, the recovery condition shows a return to the control/pre-drug condition. *D*, distribution of the mean response magnitude changes across the population of neurons for the control, gabazine (GBZ), GABA and recovery conditions, for deviant (red) and standard (blue) stimuli. *, significant differences (Friedman's test, $P < 0.01$).

Table 1. Firing rates of the standard and deviant stimuli at different conditions (spikes/stimulus)

	Standard stimuli			Deviant stimuli		
Condition (drug)	Median	25%	75%	Median	25%	75%
Control ($n = 104$)	0.32	0.12	0.63	0.88	0.43	1.46
Gabazine ($n = 80$)	0.50	0.25	1.05	1.13	0.63	1.61
GABA ($n = 84$)	0.08	0.03	0.16	0.40	0.18	0.69
Recovery ($n = 88$)	0.28	0.10	0.57	0.80	0.37	1.17

significantly ($P < 0.001$) between the groups. Dunn's method was used to compare all the conditions relative to the control group and indicated differences in the control *versus* gabazine conditions and control *versus* GABA conditions ($P < 0.05$; $Q = 5.863$ and $Q = 4.665$, respectively), but not in the control *versus* recovery conditions ($P > 0.05$; $Q = 0.784$). The same differences were observed in median values for the deviant stimuli (Friedman's test, $P < 0.001$) and confirmed with Dunn's method for control *versus* gabazine and control *versus* GABA comparisons ($P < 0.05$; $Q = 4.087$ and $Q = 5.367$, respectively), but not for the control *versus* recovery comparison ($P > 0.05$; $Q = 0.284$). The Wilcoxon signed rank test was used to compare the median firing rate for the standard and deviant conditions. In all conditions (control, gabazine, GABA and recovery) the firing rate for the deviant stimulus was significantly larger than the firing rate for the standard stimulus ($P < 0.001$ in all cases; $Z = 8.122$, $Z = 7.311$, $Z = 7.355$ and $Z = 7.637$, respectively).

The CSI value was calculated for each neuron in the control ($n = 52$) and recovery ($n = 44$) conditions, and for at least one of the two experimental conditions: (i) after gabazine application ($n = 40$), and/or (ii) after GABA application ($n = 42$). As all neurons were affected by the drug application, data were pooled regardless of CSI values. At a population level, Friedman's repeated-measures ANOVA on ranks showed significant differences between the control and both drug groups (Fig. 4*A*) (CSI median, control: 0.431; gabazine: 0.345; GABA: 0.613; recovery: 0.457; $P < 0.001$), which were confirmed using Dunn's method in the control *versus* gabazine and control *versus* GABA comparisons ($P < 0.05$; $Q = 2.41$ and $Q = 2.52$, respectively). Dunn's method did not show differences between the control and recovery conditions (Fig. 4*B*) ($P > 0.05$, $Q = 0.11$). To determine whether these significant differences between CSI values correlated with individual changes in the presence of the drugs, we used the bootstrap method over 1000 randomizations to estimate the 95% CI of the CSI in the control condition for each neuron [Fig. 4*B* (black whiskers indicate the CI)]. The analysis demonstrated that, regardless of the level of SSA, 79% of neurons analysed ($n = 41/52$) showed significant changes in SSA sensitivity (i.e. gabazine generally decreased and GABA increased the degree of SSA). The application of gabazine decreased CSI levels (Fig. 4*B*, green triangles) in 18 of 40 neurons (45%), increased CSI levels in two cases (5%), and did not change them in 20 of 40 neurons (50%). Similarly, the application of GABA increased the levels of CSI in 24 of 42 neurons (57%) (Fig. 4*B*, red circles), produced a significant decrease in five cases (12%), and caused no change in 13 cases (31%). There is a direct correlation between the change in CSI and firing rate such that the larger the change in firing rate, the larger the change in CSI, independently of the drug used (Pearson's correlation, $Q = -0.548$, $P < 0.05$). All but 11 neurons completely recovered to control values (Fig. 4*B*, cyan triangles). Across the population, GABA effects were more noticeable when the neuron initially showed low CSI levels, whereas gabazine decreased CSI mainly for neurons with larger CSI values.

Comparison of GABA and gaboxadol effects on SSA

Seven of the 52 neurons were evaluated using GABA and gaboxadol applications, making it possible to compare the effects of each (GABA activates both $GABA_A$ and $GABA_B$ receptors, whereas gaboxadol is a $GABA_A$ selective superagonist). Repeated-measures ANOVA indicated that mean values for both the standard and deviant stimuli differed significantly ($P < 0.001$) between the groups (data not shown). The Holm–Sidak method was used to make comparisons among all the conditions and established differences in the control *versus* GABA and control *versus* gaboxadol conditions for both the standard ($P < 0.05$; $t = 8.105$ and $t = 6.576$, respectively) and deviant ($P < 0.05$; $t = 5.086$ and $t = 4.222$, respectively) stimuli, but not in the GABA *versus* gaboxadol conditions ($P > 0.05$ for both standard and deviant stimuli). Repeated-measures ANOVA showed differences in CSI between the control group and both drug groups (mean ± S.D. CSI, control: 0.41 ± 0.15; GABA: 0.59 ± 0.21; gaboxadol: 0.57 ± 0.08; recovery: 0.37 ± 0.14; $P < 0.001$). Holm–Sidak *post hoc* analysis confirmed these differences but did not show any differences between the control and recovery conditions ($P > 0.05$) or the GABA and gaboxadol conditions ($P > 0.05$). The lack of differential gaboxadol action suggests that GABA's mechanism for enhancing SSA may not be mediated only by specific extrasynaptic $GABA_A$ or $GABA_B$ receptors.

Effects of gabazine and GABA on the time course of adaptation

The effects of applications of gabazine and GABA on the temporal dynamics of adaptation during the oddball

sequence were evaluated before, during and after drug application (Fig. 5). The time course of adaptation in all four conditions (control, gabazine, GABA and recovery) was fitted by a double exponential function defined as $f(t) = A_{stst} + A_r \cdot e^{-t/\tau(r)} + A_s \cdot e^{-t/\tau(s)}$ ($r^2 = 0.89$–0.95). This function contains a rapid (r) and a slow (s) component, after which the response reaches a steady state (A_{stst}). Because of its subtle adaptation, deviant tones do not fit this function (Antunes *et al.* 2010; Antunes & Malmierca, 2011). We analysed only the responses of neurons that showed significant SSA (CSI > 0.18) [control ($n = 42$), gabazine ($n = 32$), GABA ($n = 32$) and recovery ($n = 35$)] because the use of all the neurons in the population would have diluted these dynamics.

The rapid component did not show differences in the speed/time course of decay [$\tau(r)$] in the control *versus* gabazine conditions, but did reveal significant differences between the control and GABA conditions (Table 2). Moreover, there were significant differences in the magnitude of the decay of the rapid component (A_r) between the control and GABA conditions (Table 2, second column). For the slow component, the speed of decay [$\tau(s)$] in the control condition differed significantly with that in the GABA condition, but not with that in the gabazine condition (Table 2, third column). Additionally, the magnitude of decay of the slow component (A_s) was significantly lower in both the GABA and gabazine conditions (Table 2, fourth column). Interestingly, in the GABA condition, A_s was more pronounced (but the decrease smaller) than in the control condition. This correlated with the larger decrease in the response observed within the rapid component. Finally, the magnitude of the steady-state component (A_{stst}) confirmed that the response was greatly reduced in the

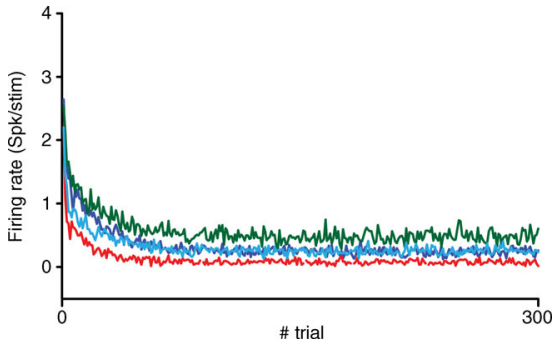

Figure 5. Time course of adaptation in medial geniculate body (MGB) neurons before, during and after the application of gabazine and GABA
Averaged population firing rate responses (spikes/stimulus) to the standard stimulus of neurons with adaptation [common specific index (CSI) > 0.18] in the control (dark blue), gabazine (green), GABA (red) and recovery (light blue) conditions.

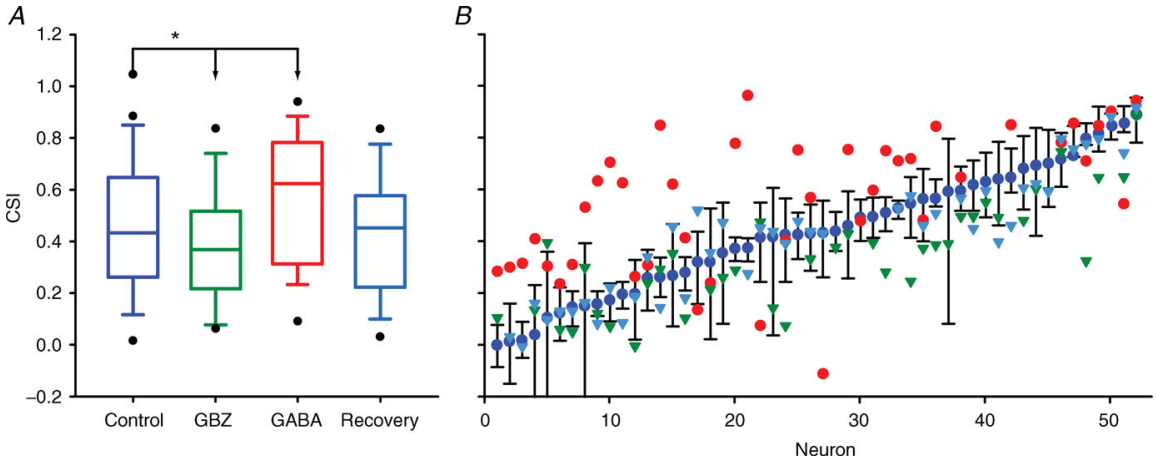

Figure 4. Stimulus-specific adaptation (SSA) quantification in medial geniculate body (MGB) neurons before, during and after the application of gabazine and GABA
A, distribution of common stimulus-specific adaptation index (CSI) values in the control (dark blue), gabazine (GBZ; green), GABA (red) and recovery (light blue) conditions for the population of neurons that responded properly considering our criteria (control: $n = 52$; gabazine: $n = 40$; GABA: $n = 42$; recovery: $n = 44$). Continuous lines across the plots represent median values. *, significant differences (between drug conditions: Friedman's test, $P < 0.01$; between standard and deviant stimuli: Wilcoxon's test, $P < 0.01$). *B*, CSI values for individual neurons in the control (dark blue circles), gabazine (green triangles), GABA (red circles) and recovery (light blue triangles) conditions. Error bars indicate the 95% confidence intervals of the control responses of each neuron calculated using bootstrapping. All dots outside error bars represent CSI values that are statistically different from those of the control condition.

Table 2. Double exponential coefficients in different conditions. Superimposition with the 95% confidence interval in the control condition indicates there are no significant differences between the groups

	Fast component		Slow component		
Condition (r^2)	Speed:τ(r) (ms)	Decay:A_r	Speed:τ(s) (ms)	Decay:A_s	Steady-state value (A_{stst})
Control (0.95)	0.96 (0.67 – 1.25)	3.02 (2.00 – 4.04)	22.38 (20.79 – 23.96)	1.37 (1.29 – 1.44)	0.28 (0.27 – 0.29)
Gabazine (0.89)	1.13 (0.71 – 1.55)	2.85 (1.80 – 3.89)	23.83 (20.98 – 26.69)	1.16* (1.05 – 1.27)	0.48* (0.47 – 0.49)
GABA (0.95)	0.54* (0.42 – 0.66)	8.14* (4.89 – 11.40)	15.69* (14.42 – 16.96)	0.83* (0.78 – 0.88)	0.06* (0.06 – 0.07)

Values are means (95% confidence intervals). *, statistical differences.

GABA condition in comparison with the control condition (in some cases GABA application completely suppressed responses to the standard tone) (Table 2, last column).

Effects of gabazine and GABA on the latency of MGB neurons

The impacts of gabazine and GABA application on first spike latency (FSL) in response to the standard and deviant stimuli were evaluated (control: 104; gabazine: 84; GABA: 80; recovery: 88). Both gabazine and GABA had a greater effect on the temporal response to deviant stimuli relative to the standard (Fig. 6; Table 3). However, no significant differences emerged between the control and drug conditions for either the standard or deviant stimuli (Friedman's test, $P = 0.169$ and $P = 0.083$, respectively). Generally, gabazine resulted in a small non-significant reduction in FSL in response to deviant stimuli (Fig. 6*A*, red dots; Table 3, fourth column), whereas GABA application increased FSL (Fig. 6*B*, red dots; Table 3, fourth column). Both gabazine and GABA minimally affected responses to the standard stimuli. Latency to deviant stimuli was significantly shorter than to standard stimuli in all but the GABA condition, in which response latencies to both stimuli were equalized (Wilcoxon signed rank test: control: $Z = -5.197$, $P < 0.001$; gabazine: $Z = -6.058$, $P < 0.001$; GABA: $Z = -1.936$, $P = 0.053$; recovery: $Z = -3.72$, $P < 0.001$).

Discussion

The present study finds that activation of $GABA_A$ receptors with GABA or the selective agonist gaboxadol results in a significant increase in the level of SSA by differentially decreasing the response rate to common stimuli and having a lesser effect on the response rate to novel stimuli. Conversely, gabazine application results in a significant decrease in SSA but increases the firing rate. In general, the increase in firing rate was larger for the standard than for the deviant stimulus. The similar effects of GABA and the $GABA_AR$ superagonist gaboxadol support the suggestion that GABA inhibition enhances SSA by acting preferentially at synaptic and to a lesser extent at extrasynaptic $GABA_A$ and $GABA_B$ receptors.

Previously, SSA has been studied using the oddball paradigm and the CSI in the MGB (Yu *et al.* 2009; Antunes *et al.* 2010; Antunes & Malmierca, 2011). For consistency, the present stimulus set was chosen to facilitate comparisons with the findings of previous studies. The present work selected pairs of frequencies close to threshold and near the high-frequency edge in order to evoke the highest possible degree of SSA (Duque *et al.* 2012). The levels of CSI found for the neurons in our dataset ($n = 52$, mean ± S.E.M. CSI: 0.443 ± 0.035; median CSI: 0.431) were similar to those in other recent MGB studies using comparable conditions (frequency contrast: $\Delta f \sim 0.1$; repetition rate: 4 Hz; deviant appearance: 10%). Yu *et al.* (2009) demonstrated weaker SSA in MGB ($n = 41$, mean ± S.E.M. CSI: 0.154 ± 0.020), but used a slower repetition rate (1 Hz) and higher intensity (70 dB SPL), which generally evokes lower SSA levels (Duque *et al.* 2012). Antunes and colleagues (2010), using conditions identical to those in the present study, found degrees of SSA that were larger in the non-lemniscal regions of the MGB (median CSI, MGV: 0.08; MGD: 0.37; MGM: 0.76).

In the present study, the increase in SSA level produced by the activation of $GABA_AR$s reflected a larger impact than that of gabazine $GABA_AR$ blockade. Even considering that these larger changes of the CSI in response to GABA, in comparison with gabazine, may be an outcome of the equation for CSI (as the spike rates to the standards approach 0 in the presence of GABA, CSI will approach 1), the observed differences are large enough to indicate that additional factors are necessary to explain this finding. These may include: (i) the presence of both synaptic and extrasynaptic $GABA_AR$ constructs; (ii) a near-threshold basal $GABA_AR$ activation state, and/or (iii) an additional effect of $GABA_B$ receptors (Luo *et al.* 2011). Findings from the present and previous studies suggest that GABA's ability to modulate SSA is likely to be mediated by $GABA_A$ rather than $GABA_B$ receptors. Gaboxadol effects no action and does not bind to $GABA_B$ receptors (Bowery *et al.* 1983). As the present results show similar effects in SSA gain after gaboxadol and GABA application, it is unlikely that these actions are

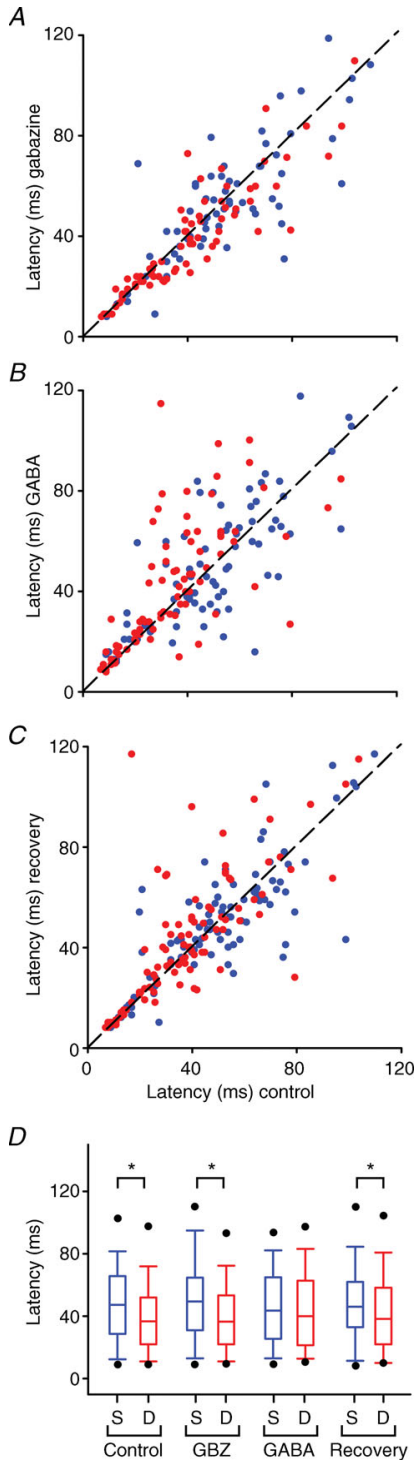

Table 3. Latencies of standard and deviant stimuli at different conditions (first spike latency)

	Standard stimuli			Deviant stimuli		
Condition (drug)	Median	25%	75%	Median	25%	75%
Control ($n = 104$)	47.3	26.0	65.8	35.8	20.9	51.9
Gabazine ($n = 80$)	49.5	29.0	65.8	29.5	21.0	51.1
GABA ($n = 84$)	43.5	25.6	65.0	40.0	21.5	62.8
Recovery ($n = 88$)	44.8	28.0	62.8	38.3	19.5	59.0

mediated through $GABA_B$Rs. In addition, the fact that gabazine does not block $GABA_B$ receptors, and exerts a qualitatively smaller reduction in SSA than does GABA, reinforces the suggestion that $GABA_B$ receptors are not prominently involved in SSA coding. A previous study demonstrated that $GABA_B$ receptor blockade significantly reduced response habituation in the superior colliculus (Binns & Salt, 1997). However, at least in rat, highest CSI values were found in MGM (Antunes *et al.* 2010), an area thought to lack $GABA_B$ receptors (Smith *et al.* 2007). With reference to (i) and (ii) above, when would an agonist be more effective than an antagonist? Relatively low endogenous levels of GABA will only activate extrasynaptic $GABA_A$Rs and, although not fully established, gabazine may require higher iontophoretic concentrations to block extrasynaptic $GABA_A$Rs relative to synaptic $GABA_A$Rs (Farrant & Nusser, 2005; Glykys & Mody, 2007). Thus, an agonist such as GABA or the selective agonist gaboxadol, acting at both synaptic and extrasynaptic $GABA_A$Rs, may be more efficacious than the less selective antagonist gabazine.

The GABAergic projection of the TRN has been proposed as important in shaping novelty detection and/or controlling gain in MGB (Yu *et al.* 2009). Cortical deactivation did not significantly impact SSA in MGB (Antunes & Malmierca, 2011), and although this manipulation does not alter the MGB–TRN–MGB inhibitory loop, it may presumably reduce the impact of the AC–TRN GABAergic input to the MGB pathway.

Figure 6. Effects of gabazine and GABA on latency responses in medial geniculate body (MGB) neurons
A–C, scatterplots showing the mean first spike latencies (latency, in milliseconds) of neurons to deviant (red dots) and standard (blue dots) stimuli in the control *vs.* gabazine (*A*), GABA (*B*) and recovery (*C*) conditions. Dots represent one of each frequency analysed separately in each pair of stimuli recorded with the oddball paradigm (52 neurons; 104 frequencies). *D*, distribution of latency values in response to standard (blue plots) and deviant (red plots) stimuli in the control, gabazine (GBZ), GABA and recovery conditions. *, significant differences (Wilcoxon's test, $P < 0.01$) for all groups except GABA, in which latency responses to both standard and deviant stimuli were equalized.

As only 1% of neurons within MGB are thought to be GABAergic (Winer & Larue, 1996), it is likely that the primary inhibitory projection impacting SSA derives from the ascending GABAergic projections from the IC (Winer *et al.* 1996) and the MGB–TRN–MGB circuits (Rouiller *et al.* 1985; Cotillon-Williams *et al.* 2008; Yu *et al.* 2009). The present data, in conjunction with those from the cortical deactivation study cited earlier (Antunes & Malmierca, 2011), support the contention that $GABA_AR$ manipulation using GABA- or gaboxadol-activated $GABA_ARs$ may mimic ascending inhibition from IC and/or the MGB–TRN–MGB inhibitory loop.

$GABA_AR$ blockade increased MGB neurons' firing rate under all conditions while decreasing CSI levels, but the temporal dynamics of adaptation were minimally affected; i.e. the adaptation function (Fig. 5) was shifted because of a general increase in firing rate. With respect to the relative impact of synaptic *versus* extrasynaptic $GABA_ARs$ on SSA, exogenous application of GABA or gaboxadol similarly decreased the firing rate under all conditions, increasing the CSI levels of the MGB. If the extrasynaptic selective $GABA_AR$ superagonist gaboxadol had shown a greater effect than GABA, this might have been speculated to be a primarily extrasynaptic $GABA_AR$ effect (Richardson *et al.* 2013*b*).

Alteration of the SSA response by $GABA_AR$ manipulation was not frequency-specific: similar effects on the SSA response were apparent over a range of frequencies. Previous studies have found that GABAergic inputs impact frequency tuning through $GABA_A$ receptors (Suga *et al.* 1997) and alter neuronal thresholds (Cotillon-Williams *et al.* 2008) of MGB neurons. In the IC, Pérez-González *et al.* (2012) observed that $GABA_AR$ manipulation altered CSI levels in a manner similar to the present MGB findings. In the present study, the GABAergic system did not generate or create SSA *de novo* in the MGB, but analogously to the effects observed in the IC (Ingham & McAlpine, 2005; Pérez-González *et al.* 2012; Pérez-González & Malmierca, 2012) and the visual cortex (Katzner *et al.* 2011), GABAergic inputs serve a significant gain control function (Robinson & McAlpine, 2009; Isaacson & Scanziani, 2011).

We found no differences in response latencies between the control condition and the gabazine and GABA conditions. Although somewhat unexpected, these results are in agreement with those of previous studies demonstrating that GABA inhibition has little effect on response latencies in the IC (LeBeau *et al.* 1996; Fuzessery *et al.* 2003; Sivaramakrishnan *et al.* 2004) and AC (Kaur *et al.* 2004). To the best of our knowledge, no latency analysis in the MGB in the presence of GABA receptor agonists or blockers has been performed previously. Interestingly, the changes in latency in those responses with control latencies lower than 30 ms appear to be much smaller than those at longer latencies. Although a detailed latency analysis of the >30 ms group does not show differences between the control and the drug groups (Friedman's test, standard stimulus: $P = 0.264$; deviant stimulus: $P = 0.035$), it is tempting to speculate about a differential GABAergic effect concerning the region of the MGB: whereas MGV has short latencies, those of the MGD and MGM are longer (Calford 1983; Calford & Aitkin 1983; Anderson *et al.* 2006; Anderson & Linden, 2011). As MGB neurons maintained a shorter latency to the deviant than to the standard stimulus (Antunes *et al.* 2010), even during cortical deactivation (Antunes & Malmierca, 2011), it is safe to conclude that the latency phenomenon is not of direct cortical origin nor directly related to GABA circuits. Moreover, as glycine is absent from the MGB (Aoki *et al.* 1988; Friauf *et al.* 1997), differential excitatory neuronal integration is the more likely candidate for regulating the latency of the response.

Taken together, these results suggest that in the MGB, $GABA_A$-mediated inhibition regulates SSA sensitivity in a gain control manner (i.e. by decreasing excitation to common stimuli while having a smaller effect on the response rate to novel stimuli and thus sharpening the contrast between them), thus demonstrating an 'iceberg effect' (Rose & Blakemore, 1974; Isaacson & Scanziani, 2011). This inhibitory effect tends to maximize the deviant to standard ratio. Assuming that excitatory inputs remain constant under the drug injections, these results may be explained by small changes that either hyperpolarize the membrane potential or increase the membrane conductance, both of which are enabled by the activation of $GABA_ARs$. As tonic hyperpolarization of the resting membrane potential is mediated through extrasynaptic $GABA_A$ receptors (Richardson *et al.* 2011, 2013*b*) and we have shown that gaboxadol (the extrasynaptic selective $GABA_AR$ superagonist) does not exert a larger effect than GABA, tonic hyperpolarization alone is not likely to explain the iceberg effect. By contrast, as GABA may also produce a non-linear effect through shunting inhibition (i.e. by altering membrane conductance) (Borg-Graham *et al.* 1998; Vida *et al.* 2006; Mann & Paulsen, 2007), this shunting inhibition may account for the iceberg effect. Similar results have been shown in the IC (Pérez-González *et al.* 2012; Pérez-González & Malmierca, 2012). The existence of consecutive gain controls over SSA in diverse auditory nuclei (IC and MGB, so far) suggests the existence of successive hierarchical levels of processing through the auditory system that would allow the reduction of redundant information. If SSA is generated in the IC (Malmierca *et al.* 2009; Ayala & Malmierca, 2013; Ayala *et al.* 2013), the first important GABAergic modulation will occur at this lowest level and will require additional adjustments as SSA is propagated up the auditory pathway through the MGB. The rat MGB contains one-fifth of the number of neurons present in the IC (Kulesza *et al.* 2002). Therefore, the role of MGB neurons may be to combine

and integrate the adaptive properties over more inputs received than do individual IC neurons. Similar ideas have been proposed (Anderson & Malmierca, 2013) for the role of the corticofugal modulation of SSA.

References

Anderson LA, Christianson GB & Linden JF (2009). Stimulus-specific adaptation occurs in the auditory thalamus. *J Neurosci* **29**, 7359–7363.

Anderson LA & Linden JF (2011). Physiological differences between histologically defined subdivisions in the mouse auditory thalamus. *Hear Res* **274**, 48–60.

Anderson LA & Malmierca MS (2013). The effect of auditory cortex deactivation on stimulus-specific adaptation in the inferior colliculus of the rat. *Eur J Neurosci* **37**, 52–62.

Anderson LA, Malmierca MS, Wallace MN & Palmer AR (2006). Evidence for a direct, short latency projection from the dorsal cochlear nucleus to the auditory thalamus in the guinea pig. *Eur J Neurosci* **24**, 491–498.

Antunes FM & Malmierca MS (2011). Effect of auditory cortex deactivation on stimulus-specific adaptation in the medial geniculate body. *J Neurosci* **31**, 17306–17316.

Antunes FM, Nelken I, Covey E & Malmierca MS (2010). Stimulus-specific adaptation in the auditory thalamus of the anesthetized rat. *PLoS One* **5**, e14071.

Aoki E, Semba R, Keino H, Kato K & Kashiwamata S (1988). Glycine-like immunoreactivity in the rat auditory pathway. *Brain Res* **442**, 63–71.

Ayala YA & Malmierca MS (2013). Stimulus-specific adaptation and deviance detection in the inferior colliculus. *Front Neural Circuits* **6**, 89.

Ayala YA, Perez-Gonzalez D, Duque D, Nelken I & Malmierca MS (2013). Frequency discrimination and stimulus deviance in the inferior colliculus and cochlear nucleus. *Front Neural Circuits* **6**, 119.

Backoff PM, Shadduck Palombi P & Caspary DM (1999). Gamma-aminobutyric acidergic and glycinergic inputs shape coding of amplitude modulation in the chinchilla cochlear nucleus. *Hear Res* **134**, 77–88.

Bartlett EL & Smith PH (1999). Anatomic, intrinsic, and synaptic properties of dorsal and ventral division neurons in rat medial geniculate body. *J Neurophysiol* **81**, 1999–2016.

Binns KE & Salt TE (1997). Different roles for $GABA_A$ and $GABA_B$ receptors in visual processing in the rat superior colliculus. *J Physiol* **504**, 629–639.

Borg-Graham LJ, Monier C & Fregnac Y (1998). Visual input evokes transient and strong shunting inhibition in visual cortical neurons. *Nature* **393**, 369–373.

Bowery NG, Hill DR & Hudson AL (1983). Characteristics of $GABA_B$ receptor binding sites on rat whole brain synaptic membranes. *Br J Pharmacol* **78**, 191–206.

Calford MB (1983). The parcellation of the medial geniculate body of the cat defined by the auditory response properties of single units. *J Neurosci* **3**, 2350–2364.

Calford MB & Aitkin LM (1983). Ascending projections to the medial geniculate body of the cat: evidence for multiple, parallel auditory pathways through thalamus. *J Neurosci* **3**, 2365–2380.

Candy JM, Boakes RJ, Key BJ & Worton E (1974). Correlation of the release of amines and antagonists with their effects. *Neuropharmacology* **13**, 423–430.

Caspary DM, Palombi PS & Hughes LF (2002). GABAergic inputs shape responses to amplitude modulated stimuli in the inferior colliculus. *Hear Res* **168**, 163–173.

Caspary DM, Schatteman TA & Hughes LF (2005). Age-related changes in the inhibitory response properties of dorsal cochlear nucleus output neurons: role of inhibitory inputs. *J Neurosci* **25**, 10952–10959.

Clerici WJ, McDonald AJ, Thompson R & Coleman JR (1990). Anatomy of the rat medial geniculate body: II. Dendritic morphology. *J Comp Neurol* **297**, 32–54.

Cotillon-Williams N, Huetz C, Hennevin E & Edeline JM (2008). Tonotopic control of auditory thalamus frequency tuning by reticular thalamic neurons. *J Neurophysiol* **99**, 1137–1151.

Duque D, Perez-Gonzalez D, Ayala YA, Palmer AR & Malmierca MS (2012). Topographic distribution, frequency, and intensity dependence of stimulus-specific adaptation in the inferior colliculus of the rat. *J Neurosci* **32**, 17762–17774.

Farrant M & Nusser Z (2005). Variations on an inhibitory theme: phasic and tonic activation of $GABA_A$ receptors. *Nat Rev Neurosci* **6**, 215–229.

Foeller E, Vater M & Kossl M (2001). Laminar analysis of inhibition in the gerbil primary auditory cortex. *J Assoc Res Otolaryngol* **2**, 279–296.

Friauf E, Hammerschmidt B & Kirsch J (1997). Development of adult-type inhibitory glycine receptors in the central auditory system of rats. *J Comp Neurol* **385**, 117–134.

Fuzessery ZM, Wenstrup JJ, Hall JC & Leroy S (2003). Inhibition has little effect on response latencies in the inferior colliculus. *J Assoc Res Otolaryngol* **4**, 60–73.

Glykys J & Mody I (2007). Activation of $GABA_A$ receptors: views from outside the synaptic cleft. *Neuron* **56**, 763–770.

Hara K & Harris RA (2002). The anesthetic mechanism of urethane: the effects on neurotransmitter-gated ion channels. *Anesth Analg* **94**, 313–318.

Hu B (2003). Functional organization of lemniscal and nonlemniscal auditory thalamus. *Exp Brain Res* **153**, 543–549.

Ingham NJ & McAlpine D (2005). GABAergic inhibition controls neural gain in inferior colliculus neurons sensitive to interaural time differences. *J Neurosci* **25**, 6187–6198.

Isaacson JS & Scanziani M (2011). How inhibition shapes cortical activity. *Neuron* **72**, 231–243.

Ito T, Bishop DC & Oliver DL (2011). Expression of glutamate and inhibitory amino acid vesicular transporters in the rodent auditory brainstem. *J Comp Neurol* **519**, 316–340.

Katzner S, Busse L & Carandini M (2011). $GABA_A$ inhibition controls response gain in visual cortex. *J Neurosci* **31**, 5931–5941.

Kaur S, Lazar R & Metherate R (2004). Intracortical pathways determine breadth of subthreshold frequency receptive fields in primary auditory cortex. *J Neurophysiol* **91**, 2551–2567.

Kulesza RJ, Viñuela A, Saldaña E & Berrebi AS (2002). Unbiased stereological estimates of neuron number in subcortical auditory nuclei of the rat. *Hear Res* **168**, 12–24.

LeBeau FE, Rees A & Malmierca MS (1996). Contribution of GABA- and glycine-mediated inhibition to the monaural temporal response properties of neurons in the inferior colliculus. *J Neurophysiol* **75**, 902–919.
Lee CC & Sherman SM (2011). On the classification of pathways in the auditory midbrain, thalamus, and cortex. *Hear Res* **276**, 79–87.
Luo B, Wang HT, Su YY, Wu SH & Chen L (2011). Activation of presynaptic $GABA_B$ receptors modulates GABAergic and glutamatergic inputs to the medial geniculate body. *Hear Res* **280**, 157–165.
Malmierca MS, Cristaudo S, Perez-Gonzalez D & Covey E (2009). Stimulus-specific adaptation in the inferior colliculus of the anesthetized rat. *J Neurosci* **29**, 5483–5493.
Mann EO & Paulsen O (2007). Role of GABAergic inhibition in hippocampal network oscillations. *Trends Neurosci* **30**, 343–349.
Näätänen R (1992). *Attention and Brain Function*. Lawrence Erlbaum, Hillsdale, NJ.
Paxinos G & Watson C (2007). *The Rat Brain in Stereotaxic Coordinates*, 6th edn. Elsevier, Amsterdam.
Pérez-González D, Hernández O, Covey E & Malmierca MS (2012). $GABA_A$-mediated inhibition modulates stimulus-specific adaptation in the inferior colliculus. *PLoS ONE* **7**, e34297.
Pérez-González D & Malmierca MS (2012). Variability of the time course of stimulus-specific adaptation in the inferior colliculus. *Front Neural Circuits* **6**, 107.
Peruzzi D, Bartlett E, Smith PH & Oliver DL (1997). A monosynaptic GABAergic input from the inferior colliculus to the medial geniculate body in rat. *J Neurosci* **17**, 3766–3777.
Richardson BD, Hancock KE & Caspary DM (2013*a*). Stimulus-specific adaptation in the auditory thalamus of young and aged awake rats. *J Neurophysiol* **110**, 1892–1902.
Richardson BD, Ling LL, Uteshev VV & Caspary DM (2011). Extrasynaptic $GABA_A$ receptors and tonic inhibition in rat auditory thalamus. *PLoS One* **6**, e16508.
Richardson BD, Ling LL, Uteshev VV & Caspary DM (2013*b*). Reduced $GABA_A$ receptor-mediated tonic inhibition in aged rat auditory thalamus. *J Neurosci* **33**, 1218–1227.
Robinson BL & McAlpine D (2009). Gain control mechanisms in the auditory pathway. *Curr Opin Neurobiol* **19**, 402–407.
Rose D & Blakemore C (1974). Effects of bicuculline on functions of inhibition in visual cortex. *Nature* **249**, 375–377.
Rouiller EM, Colomb E, Capt M & De Ribaupierre F (1985). Projections of the reticular complex of the thalamus onto physiologically characterized regions of the medial geniculate body. *Neurosci Lett* **53**, 227–232.
Sivaramakrishnan S, Sterbing-D'Angelo SJ, Filipovic B, D'Angelo WR, Oliver DL & Kuwada S (2004). $GABA_A$ synapses shape neuronal responses to sound intensity in the inferior colliculus. *J Neurosci* **24**, 5031–5043.
Smith PH, Bartlett EL & Kowalkowski A (2006). Unique combination of anatomy and physiology in cells of the rat paralaminar thalamic nuclei adjacent to the medial geniculate body. *J Comp Neurol* **496**, 314–334.
Smith PH, Bartlett EL & Kowalkowski A (2007). Cortical and collicular inputs to cells in the rat paralaminar thalamic nuclei adjacent to the medial geniculate body. *J Neurophysiol* **98**, 681–695.
Suga N, Zhang Y & Yan J (1997). Sharpening of frequency tuning by inhibition in the thalamic auditory nucleus of the mustached bat. *J Neurophysiol* **77**, 2098–2114.
Taaseh N, Yaron A & Nelken I (2011). Stimulus-specific adaptation and deviance detection in the rat auditory cortex. *PLoS One* **6**, e23369.
Ulanovsky N, Las L, Farkas D & Nelken I (2004). Multiple time scales of adaptation in auditory cortex neurons. *J Neurosci* **24**, 10440–10453.
Ulanovsky N, Las L & Nelken I (2003). Processing of low-probability sounds by cortical neurons. *Nat Neurosci* **6**, 391–398.
Vida I, Bartos M & Jonas P (2006). Shunting inhibition improves robustness of gamma oscillations in hippocampal interneuron networks by homogenizing firing rates. *Neuron* **49**, 107–117.
von der Behrens W, Bauerle P, Kossl M & Gaese BH (2009). Correlating stimulus-specific adaptation of cortical neurons and local field potentials in the awake rat. *J Neurosci* **29**, 13837–13849.
Wang H, Turner JG, Ling L, Parrish JL, Hughes LF & Caspary DM (2009). Age-related changes in glycine receptor subunit composition and binding in dorsal cochlear nucleus. *Neuroscience* **160**, 227–239.
Winer JA (1985). The medial geniculate body of the cat. *Adv Anat Embryol Cell Biol* **86**, 1–97.
Winer JA & Larue DT (1996). Evolution of GABAergic circuitry in the mammalian medial geniculate body. *Proc Natl Acad Sci U S A* **93**, 3083–3087.
Winer JA, Saint Marie RL, Larue DT & Oliver DL (1996). GABAergic feedforward projections from the inferior colliculus to the medial geniculate body. *Proc Natl Acad Sci U S A* **93**, 8005–8010.
Yaron A, Hershenhoren I & Nelken I (2012). Sensitivity to complex statistical regularities in rat auditory cortex. *Neuron* **76**, 603–615.
Yu XJ, Xu XX, He S & He J (2009). Change detection by thalamic reticular neurons. *Nat Neurosci* **12**, 1165–1170.

Additional information

Competing interests

None declared.

Author contributions

The experiments were performed in the Laboratory of Auditory Neurobiology, Department of Pharmacology, SIU School of Medicine (Springfield, IL, USA). D.M.C. and M.S.M. contributed to the conception and design of the experiments. D.D. collected and analysed the data. All authors contributed to the interpretation of the data and the writing of the paper, and approved the final manuscript for submission.

Funding

This work was supported by a National Institutes of Health grant (DC000151) to D.M.C. and the Spanish Ministry of Economy and Competitiveness (MINECO) (BFU2009-07286 and EUI2009-04083) in the frame of the ERA-NET NEURON to M.S.M. D.D. held a fellowship from the Spanish Ministry of Education and Science (Ministerio de Educación y Ciencia, MEC; BES-2010-035649).

Acknowledgements

The authors thank Dr B.D. Richardson, Dr R. Cai and L.L. Ling for their help and support.